



Queensland University of Technology
Brisbane Australia

This is the author's version of a work that was submitted/accepted for publication in the following source:

[Nguyen, Theanh, Chan, Tommy H.T., & Thambiratnam, David P.](#)
(2014)

Effects of wireless sensor network uncertainties on output-only modal-based damage identification.

Australian Journal of Structural Engineering, 15(1), pp. 15-25.

This file was downloaded from: <http://eprints.qut.edu.au/66965/>

© Copyright 2014 Engineers Australia

Notice: *Changes introduced as a result of publishing processes such as copy-editing and formatting may not be reflected in this document. For a definitive version of this work, please refer to the published source:*

<http://doi.org/10.7158/S12-041.2014.15.1>

EFFECTS OF WIRELESS SENSOR NETWORK UNCERTAINTIES ON OUTPUT-ONLY MODAL-BASED DAMAGE IDENTIFICATION

T. Nguyen^{1*}, T. H. T. Chan¹ and D. P. Thambiratnam¹

¹School of Civil Engineering and Built Environment,
Queensland University of Technology, Brisbane, Queensland, Australia.

*Email: theanh.nguyen@qut.edu.au

ABSTRACT

The use of Wireless Sensor Networks (WSNs) for Structural Health Monitoring (SHM) has become a promising approach due to many advantages such as low cost, fast and flexible deployment. However, inherent technical issues such as data synchronization error and data loss have prevented these distinct systems from being extensively used. Recently, several SHM-oriented WSNs have been proposed and believed to be able to overcome a large number of technical uncertainties. Nevertheless, there is limited research examining effects of uncertainties of generic WSN platform and verifying the capability of SHM-oriented WSNs, particularly on demanding SHM applications like modal analysis and damage identification of real civil structures. This article first reviews the major technical uncertainties of both generic and SHM-oriented WSN platforms and efforts of SHM research community to cope with them. Then, effects of the most inherent WSN uncertainty on the first level of a common Output-only Modal-based Damage Identification (OMDI) approach are intensively investigated. Experimental accelerations collected by a wired sensory system on a benchmark civil structure are initially used as clean data before being contaminated with different levels of data pollutants to simulate practical uncertainties in both WSN platforms. Statistical analyses are comprehensively employed in order to uncover the distribution pattern of the uncertainty influence on the OMDI approach. The result of this research shows that uncertainties of generic WSNs can cause serious impact for level 1 OMDI methods utilizing mode shapes. It also proves that SHM-WSN can substantially lessen the impact and obtain truly structural information without having used costly computation solutions.

KEYWORDS

Wireless Sensor Networks (WSNs); Structural Health Monitoring (SHM); uncertainties; generic; SHM-oriented; Data Synchronization Error (DSE); Output-only Modal Analysis (OMA); Output-only Modal-based Damage Identification (OMDI)

1. INTRODUCTION

The use of Wireless Sensor Networks (WSNs) for vibration-based Structural Health Monitoring (SHM) has increasingly become popular due to many features such as low cost, fast and flexible deployment. Moreover, this sensing technology is capable of processing data at individual nodes and therefore enabling each measurement point to be a mini intelligent monitoring station (Lynch and Loh, 2006). As a result, many WSNs have been proposed for SHM applications and their capacity and features can be found in several comprehensive reviews (Lynch and Loh, 2006; Rice and Spencer, 2009). In more recent time, SHM research community has paid more attention on commercial WSN platforms as they offer modular hardware and open software which can be further customized with ease to meet requirements of SHM applications.

However, the use of WSNs for SHM poses a number of technical challenges. Most commercial WSNs have been initially designed for generic purposes rather than SHM (Ruiz-Sandoval et al., 2006). As a result, there are many limitations of such a generic platform such as low-sensitivity sensors, high noise, poor resolution of analog-digital converters, inaccurate synchronization and unreliable data transmission (Spencer et al., 2004). Some typical examples can be seen in the cases of the generic version of the Mica or Imote2 WSNs, i.e. using their basic sensors and sensor boards (Ruiz-Sandoval et al., 2006; Rice and Spencer, 2009). Realizing such limitations, a number of research centers have begun enhancing capacity of selective WSN models in order to align them with requirements of SHM applications. High-fidelity hardware components for SHM have been

customized and specific middleware algorithms have been written to achieve tighter network synchronization and more reliable wireless communication (Pakzad et al., 2008; Nagayama et al., 2009; Rice and Spencer, 2009). This SHM-oriented WSN platform at present can be best illustrated in the combination of Imote2-based control & communication unit with SHM-A sensor board and middleware developed by the Illinois Structural Health Monitoring Project (ISHMP, see e.g. Rice and Spencer, 2009). With belief of having overcome a large number of WSN uncertainties, these SHM-oriented WSN have been moved from laboratory applications to be deployed in real large-scale infrastructure (Pakzad et al., 2008; Jang et al., 2010).

Although SHM-oriented WSNs have achieved a number of promising results, there has been very limited validation research examining the effect of improvement of this platform in comparison with its generic counterparts from the SHM application aspect. Impact of uncertainties of both platforms has not been studied in depth, particularly with respect to very popular but demanding global SHM methods such as Output-only Modal Analysis (OMA) and Output-only Modal-based Damage Identification (OMDI). It is worth noting that, OMDI and corresponding OMA techniques, have gained more popularity in comparison to their input-output counterparts in recent years as they are more applicable for monitoring in-service civil structures such as bridges under normal traffic operation (Brincker et al., 2003).

To address this need, this article first presents a review of major uncertainties of both generic and SHM-oriented WSN platforms and their effects on the most popular OMA and OMDI techniques from prior studies. Then, effects of the most inherent uncertainty are investigated with respect to the outcome of a common level 1 OMDI approach, i.e. detecting the presence of structural damage based on the deviation of modal parameters estimated by two most popular OMA techniques. The OMA techniques adopted herein are Frequency Domain Decomposition (FDD) and Data-driven Stochastic Subspace Identification (SSI-data) based on the fact that they have been considered as the most robust technique in either frequency domain or time domain and they can well complement each other. For the sake of completeness, FDD, SSI-data and their corresponding level 1 OMDI approach are also described in brief in one of the following sections. Effect of WSN uncertainties on higher levels of the OMDI approach will be addressed in future work. As being the most advanced WSN, Imote2 and its customized hardware and software as previously mentioned are selected as the representative for the SHM-oriented WSN platform in this study.

2. MAJOR UNCERTAINTIES OF GENERIC AND SHM-ORIENTED WSNs

There are a number of technical uncertainties or challenges that have been identified by prior studies (Spencer et al., 2004; Lynch and Loh, 2006). However, from a perspective of the most popular SHM methods, two major and distinct WSN uncertainties that can directly degrade data quality are data synchronization error and data loss (Nagayama et al., 2007). A brief review regarding these two factors in both generic and SHM-oriented WSN platforms and the effort of the SHM research community to address the associated issues are presented below.

Data loss is one intrinsic uncertainty in the generic WSN platform due to two main factors, viz. poor radio signal and packet collision. Sources of the first factor include excessive range of communication (i.e. too far distance between communicating nodes) with limited on-board antenna capacity and interference of environmental factors that can obstruct or degrade the radio signal. Examples for the latter case are the presence of other wireless communication systems or certain building materials like steel (Rice and Spencer, 2009). Data loss due to packet collision occurs when multiple nodes attempt to send data at the same time leading to inference between packets. Prior studies have shown that data loss in generic WSNs can be as large as 20 to 30 percent. In SHM-oriented WSNs, there are both hardware and software solutions to mitigate effects of this uncertainty. External antennas have helped SHM-oriented Imote2 sensors to increase the communication range three times compared to its generic model (Rice and Spencer, 2009). The use of external antennas has also proved to exhibit more consistent behavior with different communication distances. In the software aspect, several reliable communication protocols have been developed in middleware services so that lost data packets can be resent (Mechitov et al., 2004; Nagayama et al., 2009). With such efforts, wireless data transmission without loss is currently achievable though it has not been available in a real-time manner.

Data Synchronization Error (DSE) is probably the most well-known uncertainty in WSNs which consists of two main components, namely initial DSE and jitter-induced DSE. Major sources of initial DSE include the timing offset among local clocks of nodes and the random delay in start time of sensing in each sensor node (Nagayama et al., 2009). Jitter-induced DSE is mainly due to (1) clock drift, (2) fluctuation in sampling frequency of each sensor node and (3) difference in sampling rate among sensor nodes. The combination of the timing offset and clock-drift-induced DSE has been well known as Time Synchronization Error (TSE) which only reflects part of

DSE. In the generic WSN platform, DSE varies significantly from model to model and previous reviews (Lynch and Loh, 2006; Rice and Spencer, 2009) have reported fairly large initial DSE values in order of tens to a hundred of milliseconds for relatively limited communication ranges. Lynch et al. (2005) commented that initial DSE might become larger when a longer transmission range is in use. Clock drift rate difference among nodes can be as large as fifty microseconds per second (Nagayama et al., 2009). It might be worth noting that the total DSE of one sensing segment can be seen as the initial DSE of the next segment (Yan and Dyke, 2010). These mean that DSE could become much larger in practical data acquisition for SHM which can be as long as tens of minutes or more. In the SHM-oriented WSN platform, there are a number of solutions in both hardware and software customization efforts to cope with DSE. Rice and Spencer (2009) have customized a multi-metric sensor board named SHM-A in order to effectively mitigate the second and third source of incremental DSE. The first source of incremental DSE, clock drift, can be effectively dealt with using clock drift compensation algorithm in the time-stamping process during sensing (Nagayama et al., 2009). As a result, the remaining synchronization error for SHM-oriented Imote2 platform is mainly initial DSE which is random in range of a single sampling period (Linderman et al., 2011). Even though a lower initial DSE can be further achieved with re-sampling algorithm (Nagayama et al., 2009), this algorithm can cost more computation effort at leaf nodes and increase the data transmission latency. Tolerance capacity of SHM applications with respect to relatively small DSE in SHM-oriented WSNs needs to be assessed in order to avoid unnecessarily excessive computational and latent burden.

There are limited studies that have investigated effects of DSE on SHM applications and almost all of them have focused on effects of DSE on limited aspects of outcomes of several OMA and OMDI techniques. The rationale for such studies is, as global SHM methods, OMA and OMDI generally require data from different measurement points to be well-synchronized with each other (Nagayama et al., 2007). It is worth noting that this requirement can be easily met in the traditional wired sensing system but not in case of WSNs with inherent synchronization errors. Nagayama et al. (2007) noted substantial effects of initial DSE on modal phases estimated from one time domain on correlation functions of responses. On the other hand, Krishnamurthy et al. (2008) observed considerable influence of initial DSE on mode shape magnitudes estimated by FDD from experimental data with artificial introduction of DSE. Later, Yan and Dyke (2010) confirmed effects of DSE on both components of mode shapes and one OMDI method employing one flexibility-based index. All these three investigations have concluded that, DSE has no impact on modal frequencies and damping ratios estimated in the adopted OMA techniques. It is also notable in the latter investigation (Yan and Dyke, 2010) that DSE was randomly contaminated into different sensing nodes within a pre-determined range. This type of simulation can be seen to partially reflect the nature of DSE in WSNs, i.e. randomly different for different measurement points. However, since no multiple-round simulations have been made in this work, statistical properties of impact of DSE randomness on modal parameters and modal-based damage indices have not been derived. In addition to investigations that have been made for nonparametric and correlation-driven OMA, influence of DSE on commonly-used data-driven techniques such as SSI-data needs to be assessed. Finally, although DSE has been greatly reduced in SHM-oriented WSN platform, there appears no comparative study which has been made to evaluate effects of this improvement from a perspective of one OMDI approach. These issues will be addressed later in this study.

3. OMA AND LEVEL 1 OMDI APPROACH UNDER INVESTIGATION

Representing for non-parametric OMA is Frequency Domain Decomposition (FDD), proposed by Brincker et al. (2000). This technique starts with estimation of output power spectral density matrices each of which (G_{yy}) at a discrete frequency ω_i is then decomposed by the Singular Value Decomposition (SVD) algorithm as below

$$G_{yy}(j\omega_i) = U_i S_i U_i^H \quad (1)$$

Here, U_i is a unitary matrix containing singular vectors u_{ij} as columns and S_i is a diagonal matrix containing singular values (s_{ij}). Next, singular value lines are formed by assembling s_{ij} for all discrete frequencies of interest and plotted for implementing peak-picking technique (see Figure 2 for illustration). A mode is generally estimated as close as possible to the corresponding resonance peak of the first singular value line where the influence of the other modes is as small as possible. In the case of two orthogonally coupled modes at one frequency, the previous step is for the stronger mode whereas a peak on the second singular value line will be “picked” for the weaker mode (SVS, 2011). Mode shapes are finally derived from singular vectors corresponding to selected frequencies.

There are two variants of this technique, i.e. Enhanced FDD and Curve-fit FDD but these techniques work similarly except for the fact that estimation of damping ratios is only implemented in the two variants. Similar to

traditional input-output non-parametric techniques, FDD family is said to be fast, simple and user-friendly as well immune to computational modes (Zhang et al., 2005). However, difficulties may be arisen in the case that dense and close modes are simultaneously present.

On the other hand, Data-driven Stochastic Subspace Identification (SSI-data) has been considered as one of the most robust techniques in time domain since it can take into account furious modes from measurement noise; cope well with dense and closely spaced modes and avoid spectrum leakage (Brincker et al., 2001; Zhang et al., 2005). This method relies on directly fitting parametric state space models to the measured responses of a linear and time invariant physical system (Overschee and Moor, 1996; SVS, 2011)

$$\left. \begin{aligned} x_{t+1} &= Ax_t + w_t \\ y_t &= Cx_t + v_t \end{aligned} \right\} \quad (2)$$

Here, x_t and y_t are the state vector and the response vector at time t , respectively. A is the system state matrix whereas C is the observation matrix. Amongst two stochastic processes, w_t is the process noise (i.e. the input) that drives the system dynamics whilst v_t is measurement noise of the system response.

In later phase, subspace models are first established for different dimensions up to the user-defined maximum value. Among three subspace estimation algorithms, Un-weighted Principal Component (UPC) has been used most for SSI-data of civil structures. Estimates of matrices A and C (i.e. \hat{A} and \hat{C} , respectively) are then obtained by the least square solution. By performing the eigenvalue decomposition of the system matrix (\hat{A}), its discrete poles (μ_i) and eigenvectors (Ψ) can be found as described in (Brincker and Andersen, 2006)

$$\hat{A} = \Psi[\mu_i] \Psi^{-1} \quad (3)$$

The continuous time poles and subsequently modal frequencies and damping ratios are then obtained

$$\lambda_i = \frac{\ln(\mu_i)}{\Delta t} \quad (4)$$

$$\omega_i = |\lambda_i|; f_i = \frac{|\lambda_i|}{2\pi} \quad (5)$$

$$\zeta_i = \frac{Re(\lambda_i)}{|\lambda_i|} \quad (6)$$

Where Δt is the sampling period, the subscript ‘‘i’’ is the index of modes. Mode shape matrix is finally derived from the observation matrix and eigenvectors

$$\Phi = \hat{C} \Psi \quad (7)$$

By using increasing subspace model orders, multiple sets of modal parameters for each mode are obtained and their deviation can be used to examine whether that mode is sufficient stable to be from a genuine structural pole. This leads to the extensive use of the stabilization diagram not only in SSI-data (see Figure 2 for illustration) but also in most parametric modal analysis methods. It might be worth noting that there is another SSI technique that is based on covariance of data and therefore named covariance-driven SSI but this technique is likely to confront higher computational errors due to the issue of matrix squared up in its calculation process (Zhang et al., 2005).

In practice, FDD and SSI-data have been often used together to complement each other and they are often used for OMA of real civil structures including those being sensed by WSNs (see e.g. Weng et al., 2008; Cho et al., 2010). As for other damage identification approaches, level 1 of OMDI employing these two OMA techniques address the simple but most critical question (i.e. whether the structural damage takes place) by examining changes in modal parameters (Brincker et al., 2001). In this regard, the frequency change and the deviation (from unity) of Modal Assurance Criterion (MAC, see e.g. Allemang, 2003) are frequently-used damage indices among others (Doebling et al., 1998). The increasing use of this approach for SHM employing WSNs in recent time has proved that it deserves more thorough investigations especially those related to WSN uncertainties as previously reviewed.

4. RESEARCH METHODOLOGY

To facilitate a comparative study of effects of DSE of generic and SHM-oriented WSNs on level 1 OMDI employing FDD and SSI-data, a dataset from a benchmark structure was first selected and acts as the DSE-free dataset. This dataset was subsequently polluted with random DSE within a specified range to simulate this uncertainty of both generic and SHM-oriented WSNs based on the review results of each platform. At each DSE range, this pollution process was randomly repeated fifty times to generate fifty datasets for subsequent analyses. In the simulations for SHM-oriented WSNs, DSE range was set to be within one sampling period as previously reviewed and as to relax the option of having to use the costly re-sampling algorithm. In those for generic WSNs which generally suffer from much larger errors, three DSE ranges selected are five, ten and fifteen times of the sampling period to enable the trend of effects to be quantitatively investigated. For the sake of simplicity, impact of jitter-induced DSE is excluded in this study but one can conclude that it would cause additional adverse influence in SHM applications using generic WSNs. The DSE-free data and all DSE-corrupted datasets are used as the input, for FDD and SSI-data techniques, to identify modal frequencies, mode shapes and corresponding comparative indicators. Damping ratios are not considered in this study based on the fact that their estimation with acceptable accuracy may still be uncertain in OMA and they are not among commonly-used indices for SHM (Brincker et al., 2001). In a similar fashion as for damage detection process, relative frequency change and the deviation of MAC from unity are selected as two indicators for assessing effects of different DSE ranges on level 1 OMDI herein. Details of the original dataset, simulation approach for DSE and the analysis procedure are given the following sections.

5. DESCRIPTION OF DATASETS AND ANALYSIS

5.1 The benchmark structure and datasets

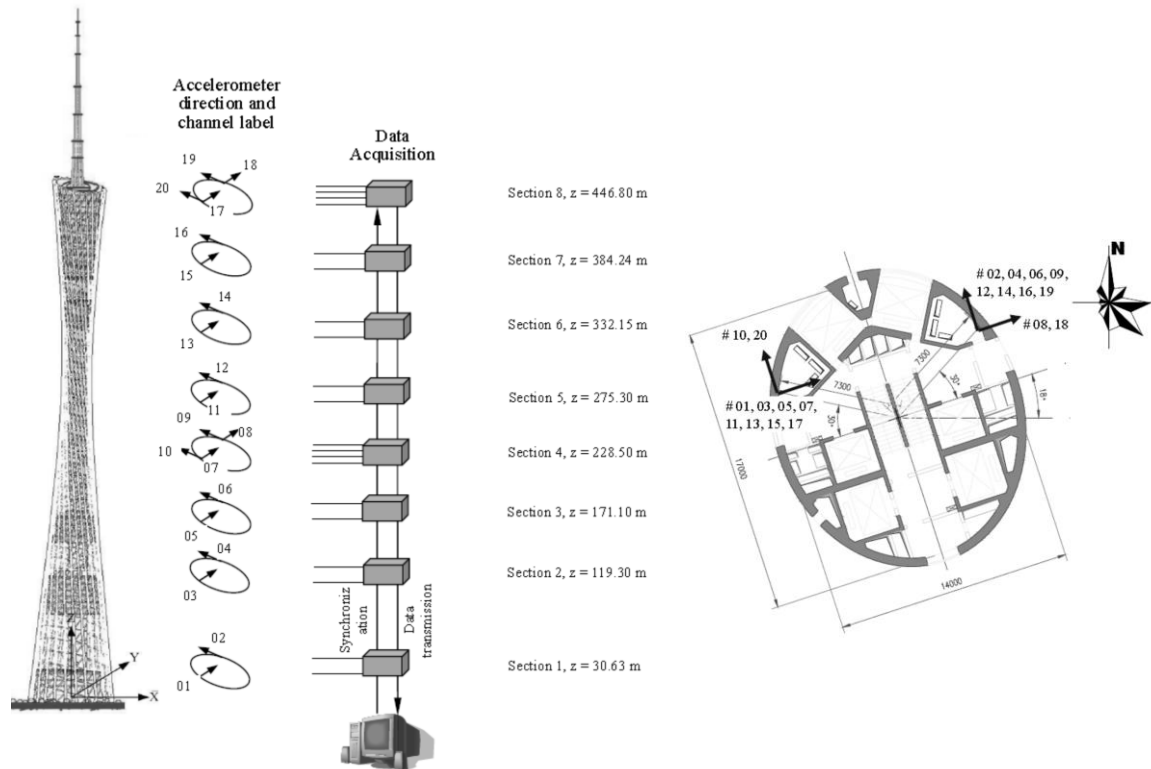


Figure 1: Position of the accelerometers and the wired data acquisition system on GNTVT

Even though simpler types of data can be generated through computer simulations or laboratory experiments, it is the intention of the authors to use real monitoring data from real civil structures in this study. The rationale for this is the pattern of real data is likely to be different from that of data generated in numerical simulations or laboratory experiments since real civil structures are subjected to influence of different operational or environmental factors such as wind and measurement noise. The dataset selected to use for this case study is from Guangzhou New TV Tower (GNTVT). This 610m super-tall tower has been considered as a benchmark structure for SHM and its one-day data as well as the full description of the SHM system are freely provided in a website for SHM research community (<http://www.cse.polyu.edu.hk/benchmark/>). Figure 1, taken from this website, shows the arrangement of 20 uni-axial accelerometers installed at eight levels along the height of this tower. Sensors were placed along short-axis and long-axis of the inner structure. The sampling rate was set at 50

samples per second which can be seen to belong to a common range for SHM of real structures. The provided data were split into 24 sets of one hour length and the 7th dataset (i.e. named `accdata_2010-01-20-00`) was chosen as benchmark (or DSE-free) dataset in this study.

5.2 Simulation of DSE and analyses of DSE impact

As previously discussed, four DSE ranges were chosen which are within one, five, ten and fifteen times of the sampling period (i.e. Δt) in which the first range represents DSE of SHM-oriented WSNs and the others represent those of generic WSNs. For a given DSE range, fifty sets of the time delay vector were randomly generated and each set was used to interpolate the corresponding DSE-corrupted dataset from the benchmark dataset. It is worth noting that, among various one-dimensional interpolation techniques, the linear interpolation technique has already been utilized in the re-sampling algorithm for SHM-oriented WSN middleware (Nagayama et al., 2009) due to the fact that it requires less computational effort from sensor resources. Since the simulations herein are not subjected to such a computational constraint, the cubic spline interpolation technique (MathWorks, 2011) was adopted to achieve more accurate simulation results.

The DSE-free and DSE-corrupted datasets were used as the input for FDD and SSI-data techniques. The analyses were conducted using ARTeMIS Extractor software ver. 5.3 (SVS, 2011). Since number of the sensors was rather large, the channel projection was adopted which can help to reduce effects of noise and avoid too much redundant cross information. The minimum number of the projection channels is generally three. The basis behind this is that, in case of two close modes, at least two projection channels are needed to separate the modes plus one additional channel to account for the measurement noise (SVS, 2011). After several trials, the number of projection channels selected was four as they provided the most stable stabilization diagram with the least noise modes. Also, the dimension for the state space model was set 160 as it was found to be sufficient for performing SSI-data. For each DSE range, fifty sets of modal parameters (i.e. frequencies and mode shapes) were estimated at each mode, compared with the benchmark modal parameter set (i.e. from the DSE-free or original dataset) to calculate fifty corresponding sets of relative frequency changes and MAC deviations from unity.

To evaluate narrow-range changes of modal parameters like frequencies, basic statistic figures are sufficient such as Root Mean Square Error (RMSE) of DSE-corrupted frequencies with respect to the DSE-free frequency and relative difference of maximum and minimum DSE-corrupted frequencies with respect also to the DSE-free frequency. In order to visualize largely different deviations of different variables in one plot, box-plot function (MathWorks, 2011) was adopted to visualize some useful statistical properties (such as median, quartiles and extremes) of MAC deviations under impact of different DSE ranges.

6. RESULTS AND DISCUSSIONS

6.1 Common results of FDD and SSI-data

The first twelve modes investigated lie on the frequency range of between 0.09 Hz and 1.3 Hz. The results of the mode estimation are in excellent agreement between both OMA techniques (i.e. FDD and SSI-data) for both DSE-free and DSE-corrupted data. MAC values of twelve mode shape vectors estimated by two techniques are approximately unity. All these twelve modes vibrate mostly along with either of two sensor-placement directions, except modes 6 and 12 which are coupled between the two directions. Figure 2 shows the singular value plot employed in FDD technique and stabilization diagram utilized in SSI-data whereas Figure 3 illustrates some typical modes vibrating mostly along with the short-axis direction (of the inner structure, see also Figure 1) for the DSE-free dataset. The results are also in good agreement with prior studies in regards to OMA of this benchmark structure (Chen et al., 2011).

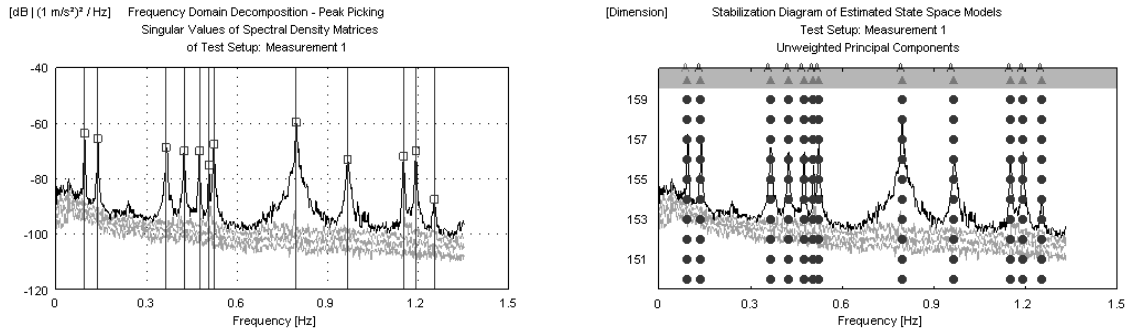


Figure 2: Singular value plot for FDD (left) and stabilization diagram for SSI-data (right) from DSE-free data

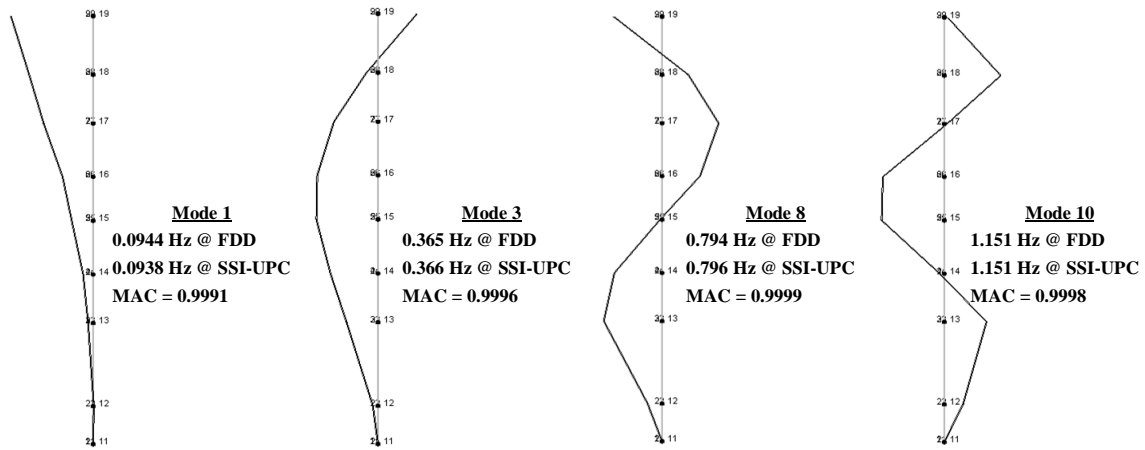


Figure 3: Four typical modes in the short axis estimated by FDD and SSI-data from DSE-free data

6.2 Effects of DSE on level 1 of OMDI

6.2.1 Frequency change

There is no change in frequencies estimated by FDD for both DSE-free and DSE-corrupted data. This once again reinforces prior findings that DSE does not affect frequencies estimated by FDD (Krishnamurthy et al., 2008; Yan and Dyke, 2010) and highlights the robustness of this technique with respect to DSE impact.

Frequency estimates by SSI-data are subjected to certain influence from DSE but the impact is very small even for the case of the largest DSE considered such as 15dt as illustrated in Table 1. The maximum RMSE, occurred at the highest mode of interest (mode 12) is only 0.392×10^{-3} Hz where as the maximum relative difference is less than 0.5 percent. Therefore, effects of DSE on frequency estimates by SSI-data can apparently be considered to be negligible.

Table 1: Effects of DSE of 15dt on frequency estimates by SSI-data

Mode	DSE-free (Hz)	RMSE ($\times 10^{-3}$ Hz)	Min (Hz)	Max (Hz)	Relative difference (%)
1	0.0938	0.123	0.0938	0.0935	0.367
2	0.1382	0.079	0.1382	0.1380	0.121
3	0.3661	0.051	0.3661	0.3660	0.032
4	0.4241	0.030	0.4241	0.4240	0.023
5	0.4748	0.036	0.4749	0.4748	0.017
6	0.5060	0.089	0.5061	0.5058	0.050
7	0.5228	0.017	0.5228	0.5227	0.015
8	0.7957	0.266	0.7958	0.7951	0.082
9	0.9663	0.022	0.9664	0.9663	0.010
10	1.1509	0.044	1.1510	1.1508	0.013
11	1.1916	0.034	1.1917	1.1916	0.012
12	1.2520	0.392	1.2525	1.2509	0.127

(Note: Relative difference = (Max-Min)/DSE-free)

6.2.2 Mode shape change - MAC deviation (from unity)

At each DSE range for one OMA technique, a 50×12 (number of simulations/observations \times number of modes) matrix of MAC deviations from unity was established and visualized by the box-plot function. To facilitate a complete comparison across different DSE ranges and with respect to two OMA techniques, a total of 8 box-plots are illustrated with the same scale in Figure 4 (for generic WSNs) and Figure 5 (for SHM-oriented WSNs). However, MAC deviations for the latter (i.e. SHM-oriented WSNs) case were re-plotted in a zoomed scale in Figure 6 to have a clearer view of their statistical distribution.

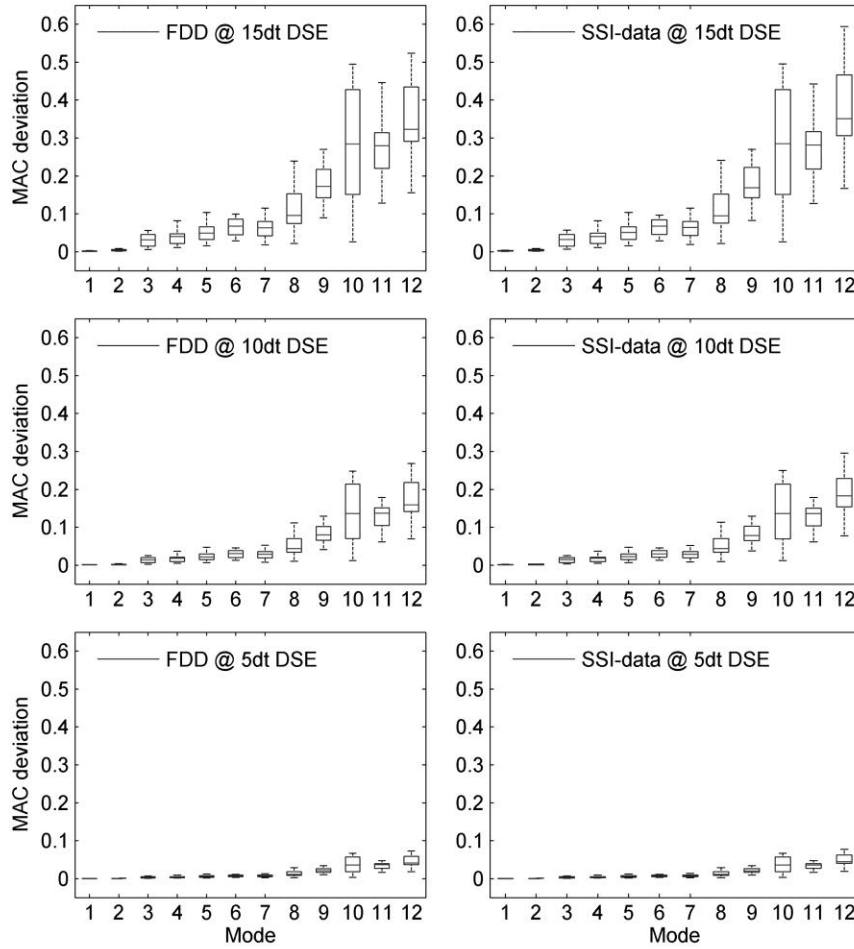


Figure 4: Box-plots of MAC deviation under DSE of generic WSN

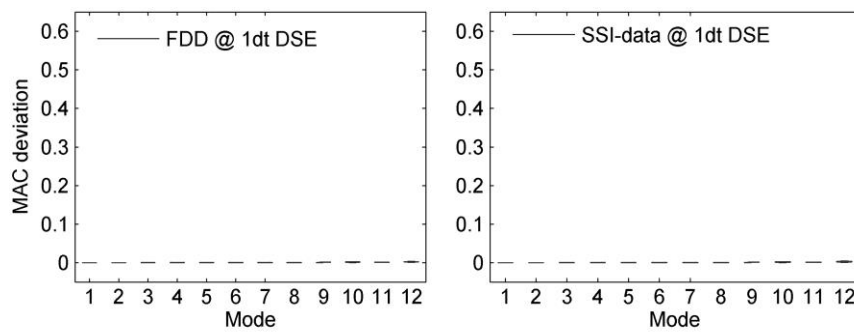


Figure 5: Box-plots of MAC deviation under DSE of SHM-oriented WSNs

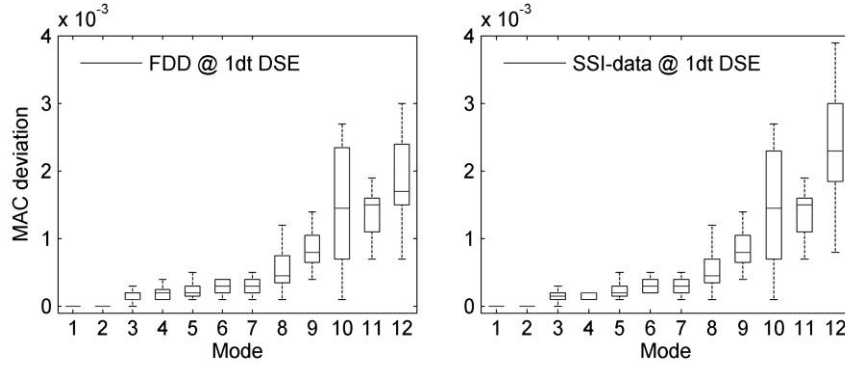


Figure 6: Box-plots of MAC deviation under DSE of SHM-oriented WSNs (zoomed scale)

Figure 4 and Figure 5 clearly show the negative impact of DSE of generic WSNs which increases rapidly for higher DSE ranges especially for higher modes. For instance of modes 10 and 11, whilst the median of MAC deviations under DSE range of 5dt is only about 0.05, those under DSE of 10dt and 15dt are around 0.13 and 0.28, respectively. Also, the variation of MAC deviations at higher DSE ranges is much larger than that at the lower range, again particularly at higher modes. This can be obviously seen through the total range (i.e. distance between the lower and upper extremes) as well as the Inter-Quartile Range (IQR) which is the difference between the 75th and 25th percentile of the presented data. For instance of modes 8 and 9, IQR of MAC deviations under DSE range of 5dt is approximately 0.15, those under DSE ranges of 10dt and 15dt are around 0.35 and 0.8, respectively. MAC deviations as large as from 0.2 to 0.35 or even larger for extreme cases (i.e. almost up to 0.6) would cause problems for level-1 OMDI relying on mode shape changes since 0.2 is also the MAC deviation (of the highest detectable mode) for the most severe damage cases in a real bridge (Brincker et al., 2001).

In general, DSE impact on statistical features of MAC deviations such as their median value and their variation is higher for higher modes. This trend can be seen not only on plots for cases of generic-WSN DSE but also on the zoomed plots (i.e. Figure 5) for the case of SHM-oriented DSE for both OMA techniques. However, for the latter case, the actual impact magnitude is drastically reduced with even the highest extreme value of MAC deviations being less than 0.005 (i.e. at mode 12). Obviously, this impact level can be considered to be marginal in comparison with those levels which have been discussed above and it also shows that OMDI is likely to tolerate the DSE level of SHM-oriented WSN without having to use costly computational algorithm like re-sampling approach.

Under adverse influence of DSE, outcomes of FDD and SSI-data are generally rather similar though one could see higher impact on SSI-data at the highest mode (i.e. mode 12). The robustness of SSI-data herein once again evidences why this technique has been believed to be the best choice for accurate OMA in both off-line and automate manner (Brincker et al., 2001).

7. CONCLUSIONS

This article has presented a comprehensive investigation of uncertainties of both generic and SHM-oriented WSN platform and their effects on a common level 1 OMDI approach. Based on an intensive review, this study has first revealed that whilst data loss can be effectively treated using reliable communication protocols, DSE is still unavoidable and can be considered as the most inherent uncertainty. The review has also shown that the DSE magnitude has been considerably alleviated in the SHM-oriented WSN platform by advanced combination of hardware and middleware solutions, and will possibly help avoiding the use of costly computational methods for compensation of DSE impact. To evaluate such improvements in SHM-oriented WSNs as well as highlight the limitation of the generic WSN platform, a comparative study was carried out with focus on applications on real civil structures. One experimental dataset from a benchmark structure was first selected to act as uncertainty-free data before being contaminated with different levels of DSE in random manners to practically simulate this uncertainty in both WSN platforms. In order to gain a more thorough understanding of DSE impact, statistical analyses, for the first time, were employed to derive critical distributions and variation patterns of two common level-1 OMDI indices i.e. frequency changes and MAC deviations from unity. The results have first shown that, the robustness of SSI-data with respect to DSE impact can be more or less the same as that of FDD. In terms of damage indices, the frequency-based index is the most robust one since DSE causes no (or almost no)

change for frequency estimates. However, the second index (i.e. MAC deviation which is commonly used for assessing mode shape change) has subjected to rather significant influence from DSE, particularly with large DSE ranges of generic WSNs. Likewise; this impact has been shown to be increased with the order of modes, proving that higher modes are more sensitive to DSE. In the same regard, capacity of SHM-oriented WSN platform has been assessed and shown that its improvement has greatly lessen the adverse impact of DSE and that OMDI is likely to perform well with data from SHM-oriented WSNs. It is also worth noting that although the effects of uncertainties like DSE on OMDI have just been investigated for level 1, the outcomes of this study can act as basis for further investigations on higher levels of OMDI. As the final finding from this study, statistical approach is ultimately recommended for investigations of WSN uncertainties particularly for data synchronization errors of generic WSNs. Beside basic statistical feature such as RMSE or relative difference, box-plots have been proved to be useful in presenting, in one plot, different variables with variations in rather different scales.

ACKNOWLEDGMENTS

The first author gratefully appreciates the financial support for his research from Vietnamese Government and Queensland University of Technology (QUT). Useful discussions with Dr Kirill Mechitov (University of Illinois at Urbana-Champaign) and Dr Tomonori Nagayama (University of Tokyo) are also acknowledged with thanks.

REFERENCES

- Allemang, R. J. 2003. The modal assurance criterion—twenty years of use and abuse. *Sound and Vibration* 37 (8):14-23.
- Brincker, R. and Andersen, P. 2006. Understanding stochastic subspace identification. In *Proceedings of the 24th International Modal Analysis Conference (IMAC), February, 2006*. St. Louis, Missouri, USA: Society for Experimental Mechanics, Inc (<http://sem-proceedings.com/24i/sem.org-IMAC-XXIV-Conf-s10p01-Understanding-Stochastic-Subspace-Identification.pdf>).
- Brincker, R., Andersen, P. and Cantieni, R. 2001. Identification and level I damage detection of the Z24 highway bridge. *Experimental Techniques* 25 (6):51-57.
- Brincker, R., Ventura, C. and Andersen, P. 2003. Why output-only modal testing is a desirable tool for a wide range of practical applications. In *Proceedings of the 21st International Modal Analysis Conference (IMAC), February, 2003, Kissimmee, Florida, USA*, pp. 1-8.
- Brincker, R., Zhang, L. and Andersen, P. 2000. Modal identification from ambient responses using frequency domain decomposition. In *Proceedings of the 18th International Modal Analysis Conference (IMAC), February, 2000, San Antonio, Texas, USA*, pp. 625-630.
- Chen, W. H., Lu, Z. R., Lin, W., Chen, S. H., Ni, Y. Q., Xia, Y. and Liao, W. Y. 2011. Theoretical and experimental modal analysis of the Guangzhou New TV Tower. *Engineering Structures* 33 (12):3628-3646.
- Cho, S., Jo, H., Jang, S., Park, J., Jung, H. J., Yun, C. B., Spencer, B. and Seo, J. W. 2010. Structural health monitoring of a cable-stayed bridge using wireless smart sensor technology: data analyses. *Smart Structures and Systems* 6 (5-6):461-480.
- Doebling, S. W., Farrar, C. R. and Prime, M. B. 1998. Summary review of vibration-based damage identification methods. *Shock and Vibration Digest* 30 (2):91-105.
- Jang, S., Sim, S. H., Jo, H. and Spencer, B. F. eds. 2010. Decentralized bridge health monitoring using wireless smart sensors. *Sensors and Smart Structures Technologies for Civil, Mechanical, and Aerospace Systems 2010, March 8, 2010 - March 11, 2010*. San Diego, CA, United states: SPIE.
- Krishnamurthy, V., Fowler, K. and Sazonov, E. 2008. The effect of time synchronization of wireless sensors on the modal analysis of structures. *Smart Materials and Structures* 17 (Compendex).
- Linderman, L. E., Mechitov, K. A. and Spencer, B. F. 2011. *Real-Time Wireless Data Acquisition for Structural Health Monitoring and Control*. Vol. 29, *NSEL Report*: University of Illinois at Urbana Champaign. <http://www.ideals.illinois.edu/handle/2142/25420>.
- Lynch, J. P. and Loh, K. J. 2006. A summary review of wireless sensors and sensor networks for structural health monitoring. *Shock and Vibration Digest* 38 (2):91-128.
- Lynch, J. P., Wang, Y., Law, K. H., Yi, J. H., Lee, C. G. and Yun, C. B. eds. 2005. Validation of a large-scale wireless structural monitoring system on the Geumgang Bridge.
- MathWorks. 2011. *MATLAB® R2011a Help Browser*. <http://www.mathworks.com/>.
- Mechitov, K., Kim, W., Agha, G. and Nagayama, T. eds. 2004. High-frequency distributed sensing for structure monitoring: Citeseer.
- Nagayama, T., Sim, S. H., Miyamori, Y. and Spencer, B. F. 2007. Issues in structural health monitoring employing smart sensors. *Smart Structures and Systems* 3 (3):299-320.

- Nagayama, T., Spencer, B. F., Mechitov, K. A. and Agha, G. A. 2009. Middleware services for structural health monitoring using smart sensors. *Smart Structures and Systems* 5 (2):119-37.
- Overschee, P. V. and Moor, B. D. 1996. *Subspace Identification for the Linear Systems: Theory-Implementation-Applications*. Kluwer Academic Publishers.
- Pakzad, S. N., Fenves, G. L., Kim, S. and Culler, D. E. 2008. Design and implementation of scalable wireless sensor network for structural monitoring. *Journal of Infrastructure Systems* 14 (Compendex):89-101.
- Rice, J. A. and Spencer, B. F. 2009. *Flexible smart sensor framework for autonomous full-scale structural health monitoring*. Vol. 018, *NSEL Report*: University of Illinois at Urbana-Champaign,. <https://www.ideals.illinois.edu/handle/2142/13635>.
- Ruiz-Sandoval, M. E., Nagayama, T. and Spencer, B. F. 2006. Sensor development using Berkeley Mote platform. *Journal of Earthquake Engineering* 10 (Compendex):289-309.
- Spencer, B. F., Ruiz-Sandoval, M. E. and Kurata, N. 2004. Smart sensing technology: Opportunities and challenges. *Structural Control and Health Monitoring* 11 (Compendex):349-368.
- SVS. 2011. *ARTEMIS Extractor, Release 5.3, User's Manual*: Structural Vibration Solutions A/S. http://www.svibs.com/products/ARTEMIS_Extractor.aspx.
- Weng, J.-H., Loh, C.-H., Lynch, J. P., Lu, K.-C., Lin, P.-Y. and Wang, Y. 2008. Output-only modal identification of a cable-stayed bridge using wireless monitoring systems. *Engineering Structures* 30 (Compendex):1820-1830.
- Yan, G. and Dyke, S. J. 2010. Structural damage detection robust against time synchronization errors. *Smart Materials and Structures* 19 (Compendex).
- Zhang, L., Brincker, R. and Andersen, P. 2005. An overview of operational modal analysis: major development and issues. In *Proceedings of the 1st International Operational Modal Analysis Conference (IOMAC), April, 2005, Copenhagen, Denmark*, pp. 179-190.